



Thermodynamic Study of Metal Corrosion and Inhibitor Adsorption of Hexamine in Mild Steel

M. BOZORG¹, T. SHAHRABI^{1,*}, J. NESHATI² and HAMED CHAGHERVAND¹

¹Department of Materials Engineering, Faculty of Engineering, Tarbiat Modares University, Tehran, Iran

²Research Institute of Petroleum Industry (RIPI), P.O. Box 14665-137, Tehran, Iran

*Corresponding author: E-mail: tshahrabi34@modares.ac.ir

(Received: 11 October 2010;

Accepted: 20 July 2011)

AJC-10166

In this study, the hexamine adsorption and thermodynamic parameters on steel in 1M HCl solution was studied. Electrochemical impedance and polarization technique at different hexamine concentrations were done and good inhibition in presence of 700 ppm hexamine was obtained in stagnant and 25 °C. In this hexamine concentration, the calculated value of activation energy is found to be 85.2 KJ/mol. Free energy and enthalpy of the adsorption were calculated -31 and -13 KJ/mol, respectively according to Langmuir isotherms and physical adsorption. Entropy of the adsorption was calculated by thermodynamic fundamental equation as well. Moreover, kinetic adsorption of hexamine studied by impedance spectroscopy. Result showed the inhibition efficiency increased up to 90 % after 12 h. The effect of hydrodynamic conditions was studied by variation in rotating speed. The results indicated that higher rotating speed negatively affected the inhibition properties.

Key Words: Hexamine, Inhibition, Thermodynamic parameters, Hydrodynamic conditions.

INTRODUCTION

Due to vast applications of iron and its alloys in industry, great attention has been paid to studies on the corrosion of iron^{1,2}. Acid solutions are extensively used in industry, the most important of which are acid pickling, industrial acid cleaning, acid-descaling and oil well acidizing. The commonly used acids are hydrochloric acid, sulfuric acid, nitric acid, *etc.*³⁻⁶. Since these acids are aggressive, inhibitors are widely used in the corrosion protection of metals in these environments⁷⁻¹⁰.

Within the group of nitrogen containing inhibitors, amines have received considerable attention, as their protonation in acidic media yields cationic species that show good inhibitive performance for steel¹¹. Hexamine (C₆H₁₂N₄, also called hexamethylenetetramine or urotropine) is probably the most widely studied amine for this purpose¹². Corrosion inhibition by hexamine has been extensively studied, especially for dissolution of iron and iron-based alloys in acid solutions^{13,14}.

Singh *et al.*¹⁵ have observed that by increasing acid concentration, NaCl and some metal cations such as Cu²⁺, As²⁺ and Sn²⁺, the inhibition efficiency of hexamine in HCl solution has been increased. Moreover, hexamine adsorption obeys Langmuir isotherm for steel in 10 % HCl solution. In a recent study, the synergism effect between hexamine and sodium dodecylbenzenesulphonate has been investigated for steel in

sulphuric acid which it strictly followed langmuir isotherm¹¹. El-Dahan *et al.*¹⁶ have found that corrosion rate of aluminum in HCl solution containing hexamine decreased by addition of KI and CaCl₂. In the literature there are reports of improvement in the inhibitive performance of hexamine in combination with certain anions, such as Cl⁻, Br⁻, I⁻, CNS⁻ and sulfonates, on the corrosion of steel in acidic solutions^{17,18}.

In industrial environments some conditions such as temperature, hydrodynamic flow and immersion time affects the inhibition efficiency which might be either beneficial or deleterious.

Despite the wide usage of hexamine, systematic research on the effects of hydrodynamic conditions and thermodynamic parameters for this inhibitor is scarce.

In this study, consequences of changes in hexamine concentration and temperature on the inhibition efficiency of steel in 1M HCl solution were investigated and the activation energy, adsorption isotherm and thermodynamic parameters have been calculated. Furthermore, the effects of immersion time and hydrodynamic conditions on hexamine adsorption have been verified.

EXPERIMENTAL

The corrosion tests were performed with standard three-electrode glass cell with a graphite rod as counter-electrode, a saturated calomel electrode (SCE) as reference electrode and

the working electrode consisted of a hollow cylinder (2.8 cm² apparent area) the composition of which is presented in Table-1.

Element	Content (%)	Element	Content (%)
C	0.085	Cr	0.06
Si	0.04	Cu	0.18
Mn	1.20	Ni	0.11
P	0.054	Pb	0.29
S	0.33	Fe	Base

The samples were first polished to a mirror finish using 80-1000 grit emery paper, immersed in ethanol and finally rinsed with double distilled water and dried before being tested.

Electrochemical studies were carried out using a computer controlled potentiostat (PAR EG and G, Model 273A) and frequency response analyzer (EG and G 1025). Impedance measurements were conducted at open circuit potential after 2 h immersion in the frequency range of 100-10 mHz by a sine wave with an amplitude of 5mV. Corrosion rates were also obtained by Tafel technique. Quasi potentiostatic polarization curves were obtained with a sweep rate of 0.6 mV s⁻¹ in the potential range of ± 0.25 V *versus* saturated calomel electrode. The experiments were repeated to ensure reproducibility.

RESULTS AND DISCUSSION

Effect of concentration: Fig. 1 shows the Nyquist plots of the mild steel samples in the presence of different concentrations of hexamine under static conditions in 1M hydrochloric acid. It is clear that the corrosion resistance of the steel samples increase with higher inhibitor concentration.

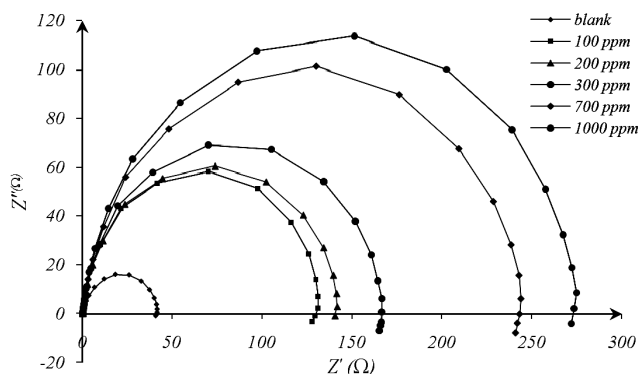


Fig. 1. Nyquist plots for specimens in solutions containing different concentrations of hexamine under static conditions

These plots with semicircle shape are indicative of the activation-controlled nature of the reactions with single charge transfer. On the other hand, such behavior may also be attributed to frequency dispersion phenomenon triggered by various causes such as roughness, inhomogeneties of solid surfaces during corrosion¹⁹, impurities, dislocation, grain boundaries²⁰, fractality²¹, distribution of active sites, adsorption of inhibitors²² and formation of porous layers^{23,24}.

The impedance spectra for the Nyquist plots was analyzed by fitting the data to the equivalent circuit model shown²⁵ in Fig. 2. The circuit comprises of a solution resistance R_s , in

series with the parallel combination of the charge transfer resistance R_{ct} and a constant phase element (CPE), which is replaced with a double layer C_{dl} .

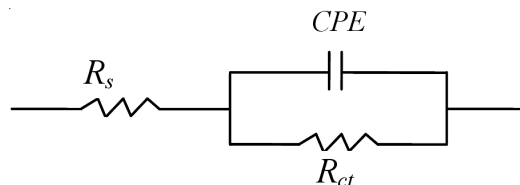


Fig. 2. Equivalent circuit used to fit the impedance spectra

Table-2 shows the impedance data for mild steel in 1M HCl in presence of different concentrations of hexamine at 25 °C after 2 h.

Concentration (ppm)	R_{ct} (Ω)	N	C_{dl} (μF cm ⁻²)
Blank	42.0	0.91	275.30
100	131.3	0.92	196.80
200	142.2	0.91	183.24
300	167.4	0.90	172.34
700	238.0	0.90	153.72
1000	272.0	0.90	146.05

As can be seen in this table the R_{ct} values increased by increasing hexamine concentration that may suggest the formation of a protective layer on the electrode surface. This layer makes a barrier for mass and charge transfer.

According to Table-2, the increase in hexamine concentration provides lower C_{dl} values, probably as a consequence of replacement of water molecules by hexamine at the electrode surface. Also it can be attributed to the decrease in local dielectric constant and/or increase in thickness of surface film layer by the adsorption of the inhibitor molecules on the metal-solution interface, according to the expression of the layer capacitance presented in the Helmholtz model²⁶:

$$C_{dl} = \frac{\epsilon \epsilon_0 A}{\delta} \quad (1)$$

where ϵ is the dielectric constant of the medium, ϵ_0 is the vacuum permittivity, A is the electrode surface area and δ is the thickness of the protective layer.

The polarization behavior of mild steel in 1M HCl in the absence and presence of different concentrations of hexamine are shown in Fig. 3. Electrochemical parameters such as corrosion current density (I_{corr}), corrosion potential (E_{corr}), Tafel slope constants (β_c and β_a) calculated from Tafel plots are given in Table-3.

E_{corr} with or without presence of different concentration of hexamine has not shown the continual and order change. This point is observed in anodic and cathodic slope. Therefore, mechanism of hexamine adsorption in 1M HCl solution can be acted as mixed inhibitor and hexamine reduces the rate of both anodic and cathodic reaction²⁷. Generally, mixed inhibitors are organic compound that reduce the rate of corrosion with adsorption on metallic surface²⁸.

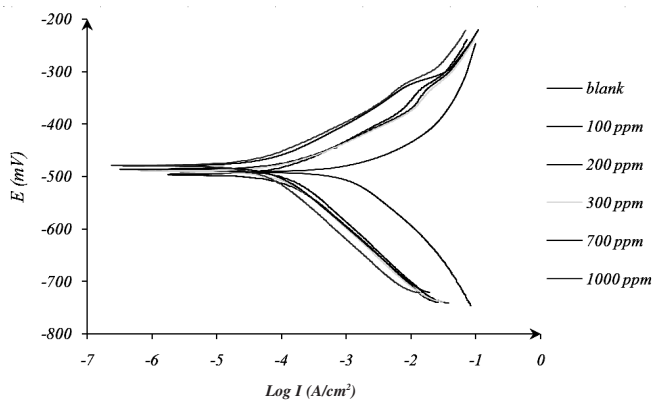


Fig. 3. Potentiodynamic polarization curves for mild steel samples in 1M HCl containing different concentrations of hexamine at 25 °C

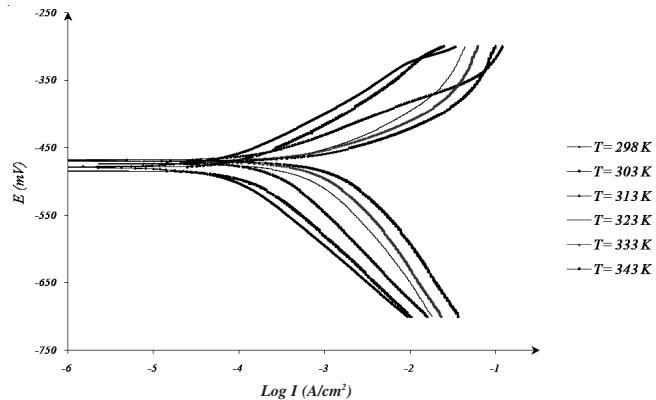


Fig. 4. Potentiodynamic polarization curves for mild steel in 1M HCl with 700 ppm hexamine at different temperatures

Concentration (ppm)	E (mv)	I _{corr} (μA/cm ²)	β _a (mV/dec)	β _c (mV/dec)	CR (mpy)
0	-489.5	572.2	112	180	92.7
100	-496.7	138.3	79.8	112.5	21.5
200	485.8	128.1	67.2	117.6	17.9
300	-490.1	100.8	55.1	109.3	15.8
700	-485.1	80.3	53.3	106.3	12.7
1000	-479.3	72.4	73.5	108.3	11.6

According to the above mentioned results and the fact that the enhancement in percentage of efficiency was negligible for the increase in inhibitor concentration from 700-1000 ppm, concentration of 700 ppm of hexamine was selected for thermodynamic and flow studies.

Effect of temperature: The importance of the correlation between the inhibition efficiency with temperature is to determine the mechanism of inhibitor adsorption on the metal surface.

In order to calculate the activation energy of the corrosion process and investigate the mechanism of inhibition, potentiodynamic polarization measurements were performed in the temperature range of 25-70 °C in the absence and presence of 700 ppm hexamine solutions.

Fig. 4 shows potentiodynamic polarization curves for the steel samples in 1M HCl containing 700 ppm hexamine in the temperature range of 25-70 °C. The corresponding results are presented in Table-4.

The results indicate that the temperature effect on corrosion rate is more pronounced for the solution with no inhibitor added compared to the solution containing inhibitor. It was also found that the efficiency of the hexamine inhibition is closely related to the temperature variation and decreases with the rise of temperature from 298-345 K.

Arrhenius equation can be exploited to explain the dependence of the corrosion rate on temperature as follows and to measure the activation energy of the metal dissolution²⁹.

$$i_{\text{corr}} = A \exp\left(-\frac{E_a}{RT}\right) \quad (2)$$

where i_{corr} is the corrosion current density, A is a constant, E_a the activation energy of the metal dissolution reaction, R is the gas constant and T is the temperature. The E_a values were calculated by the exponential regression (Fig. 5) and found to be 62.5 kJ mol⁻¹ in the uninhibited solution and 85.2 kJ mol⁻¹ in the presence of 700 ppm of hexamine. The higher E_a value in the inhibited solution can be attributed to the increased thickness of the double layer, which enhances the activation energy of the corrosion process³⁰.

Thermodynamic parameters: Adsorption on corroding surfaces never reaches real equilibrium but an adsorption steady state develops. However, when the corrosion rate is sufficiently small, the adsorption steady state has a tendency to become a quasi-equilibrium state. Thus, it is reasonable to study the quasi-equilibrium adsorption thermodynamically rather than kinetically using the appropriate equilibrium

T (K)	Concentration (ppm)	E (mV) versus SCE	I _{corr} (μA/cm ²)	β _a (mV/dec)	β _c (mV/dec)	Corrosion rate (mpy)
298	Blank	-491.7	575.2	73.5	114.8	92
	700	-483.7	80.35	68.73	106.3	12.7
303	Blank	-486.3	610	80.5	119.3	134
	700	-483	85.13	92.28	116.9	19.02
313	Blank	-479.2	1147	101.3	145.6	187
	700	-477.3	252.2	103.2	123.9	40.76
323	Blank	-474.6	3580	100.58	230.7	579
	700	-476.2	1053	107.9	180.8	170.1
333	Blank	-476.6	8764	99.2	277.4	1418
	700	-473.3	2351	102.2	182.1	380.1
343	Blank	-473.5	17222	106.6	312.8	2734
	700	-471.2	5901	102.3	231.7	937.8

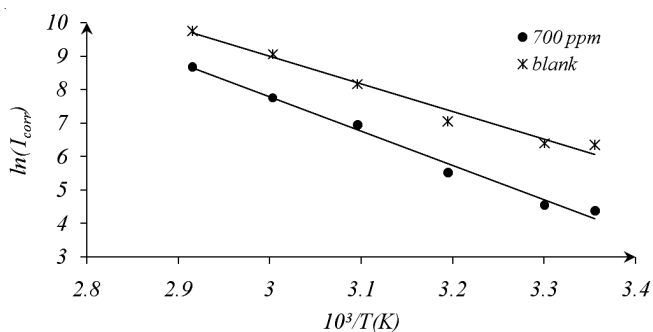


Fig. 5. Arrhenius plots for the mild steel electrode in 1M HCl

isotherms. The adsorption isotherms can provide basic information on the interaction of inhibitor and metal surface.

Langmuir, Temkin, Bockris-Swinkels, Flory-Huggins and Frumkin adsorption isotherms were verified in order to find the most suitable adsorption isotherm for hexamine on the mild steel surface in 1M HCl solution. Langmuir adsorption isotherm, which is given by eqn. 3 was found quite acceptable with an average correlation coefficient of 0.998 and the slope of 1.059 (Fig. 6).

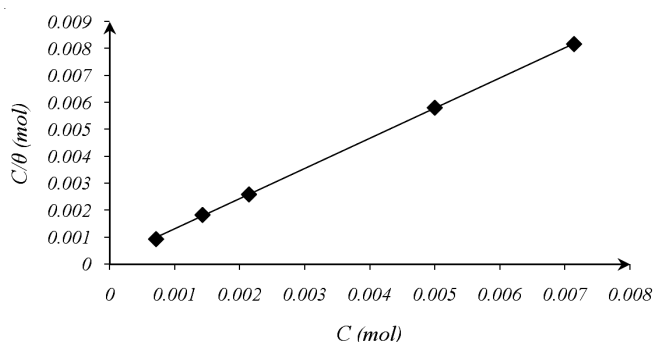


Fig. 6. Langmuir adsorption plot for the mild steel electrode in 1M HCl containing different concentrations of hexamine

$$\frac{C}{\theta} = C + \frac{1}{K_{\text{ads}}} \quad (3)$$

here C is inhibitor concentration, θ is the degree of the coverage on the metal surface and K_{ads} is the equilibrium constant for the adsorption-desorption process. Parameter θ in this equation was calculated from the following equation²⁰:

$$\theta = 1 - \frac{i_{\text{corr}}^{\text{inh}}}{i_{\text{corr}}^0} \quad (4)$$

here i_{corr}^0 and $i_{\text{corr}}^{\text{inh}}$ are the corrosion current densities in absence and presence of hexamine, respectively (Table-3).

Back to eqn. 3, the value of equilibrium constant, K_{ads} was calculated from the reciprocal of the intercept of isotherm line as $5 \times 10^{-3} \text{ L mol}^{-1}$. The free energy of the adsorption of inhibitor on mild steel surface can be evaluated³¹ by eqn. 5:

$$K_{\text{ads}} = \frac{1}{55.5} \exp\left(\frac{-\Delta G_{\text{ads}}}{RT}\right) \quad (5)$$

Knowing the value of K_{ads} , ΔG_{ads} was calculated as $-31.05 \text{ kJ mol}^{-1}$ from eqn. 5. The negative value of ΔG_{ads} reveals that the hexamine adsorption on mild steel surface is a spontaneous

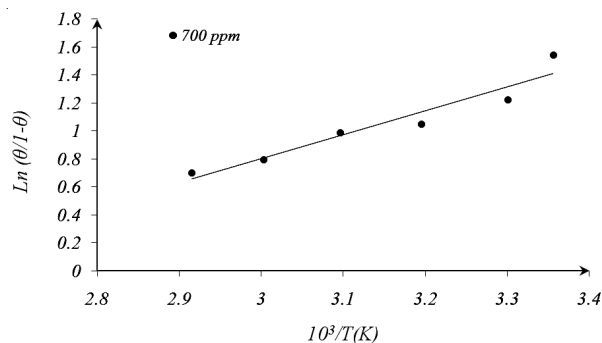
reaction and implies the strong interaction of inhibitor molecules and the metal surface. Adsorption free energy (ΔG_{ads}) values less than 40 kJ mol^{-1} is commonly interpreted by the presence of physical adsorption and formation of an adsorptive film with an electrostatic character³².

Langmuir adsorption isotherm may be expressed by the following equation³³:

$$\frac{\theta}{(1-\theta)} = AC \exp\left(\frac{-Q_{\text{ads}}}{RT}\right) \quad (6)$$

In this equation, A is a constant, Q_{ads} is the heat of adsorption and as the pressure is constant here with good approximation is equal to the enthalpy of the adsorption (H_{ads}). If the

$\ln\left(\frac{\theta}{1-\theta}\right)$ is plotted against $1000/T$ for constant hexamine concentration of 700 ppm the slope of the linear part of this curve gives the value of $\frac{-\Delta H_{\text{ads}}}{2.303R}$ and ΔH_{ads} calculated to be $-30.93 \text{ kJ mol}^{-1}$ (Fig. 7). The negative sign of ΔH_{ads} indicates that the adsorption of hexamine on the mild steel surface in 1M HCl solution is exothermic³⁴.

Fig. 7. Plot of $\ln(\theta/(1-\theta))$ versus $1000/T$ for steel sample in HCl solution with 700 ppm hexamine

Entropy of inhibitor adsorption (ΔS_{ads}) can be calculated using the second law of thermodynamics:

$$\Delta G_{\text{ads}} = \Delta H_{\text{ads}} - T\Delta S_{\text{ads}} \quad (7)$$

From eqn. 7, the value of ΔS_{ads} was found to be $53.57 \text{ J mol}^{-1} \text{ K}^{-1}$. The positive value of ΔS_{ads} is related to a mechanism called substitutional adsorption. Increase in disorder due to desorption of more water molecules³⁵, the increase in the solvent entropy and more positive water desorption entropy are among other explanations for observed sign of the entropy.

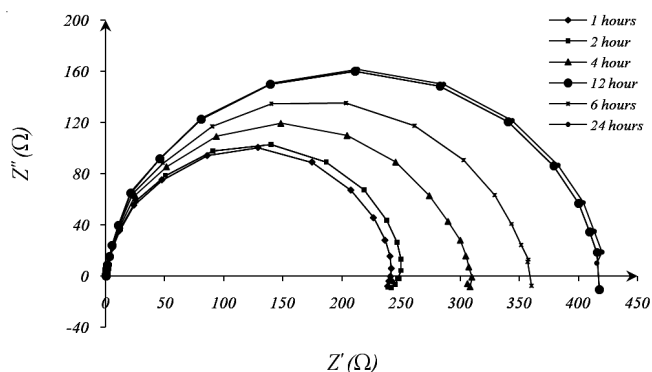


Fig. 8. Effect of immersion time on Nyquist plot of mild steel specimens in presence of 700 ppm hexamine

Effect of immersion time: Effect of immersion time study is a useful technique to determine the effectiveness of inhibition. As can be seen in Fig. 9 the inhibition effectiveness of hexamine was reached a maximum after 24 h. Obviously, the adsorption of hexamine molecules reduces the anodic dissolution reactions on metal surface in areas where it is exposed to the corrosive media.

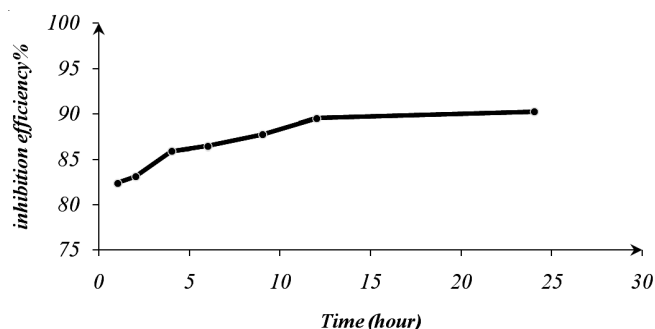


Fig. 9. Change of inhibition efficiency with immersion time for hexamine in 1M HCl

Fig. 10 shows reaction pathways of mild steel in HCl solution with and without inhibitor. When mild steel is immersed in the HCl solution, in the presence of hexamine, less hydrated chloride ions are the first chemical species adsorbed to the metal surface. Adsorbed chloride ions create an excess negative charge gradient towards the solution (step a), a condition which favours further adsorption of the cations³⁶. Protonated inhibitor hexamine molecules are adsorbed on metal surface *via* Cl⁻ ions of step a, which form interconnecting bridges between the metal atoms and the organic cations (step e). So it can be proposed that, reaction pathway of hexamine is seems to be through (a → e). The equilibrium constant k_2 must be much more bigger than k_4 ($k_2 \gg k_4$) in other words reaction (a → e) should be more favoured than (a → d). Thus, the inhibitor molecules by forming a film may act as a barrier against corrosion of the iron.

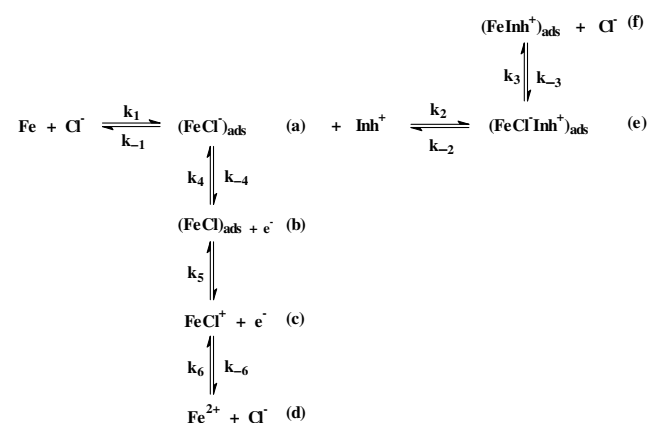


Fig. 10. Reaction pathways for Fe in HCl solution with and without inhibitor

The time dependencies of Nyquist diagrams for steel specimens in 1M HCl solution in the absence and presence of 700 ppm hexamine were shown in Fig. 8.

The change of inhibition efficiency (IE) with immersion time was given in Fig. 9. The R_{ct} values were used to calculate the inhibition efficiencies, (IE %), using the relation:

$$\text{Inhibition efficiency (\%)} = \left(1 - \frac{R_{\text{ct}}^t}{R_{\text{ct}}^0} \right) \times 100 \quad (8)$$

R_{ct}^t and R_{ct}^0 are the charge transfer resistances between solution and metal surface after t hours immersion in 1M HCl solution in presence of 700 ppm hexamine and its absence, respectively.

In the case of hexamine molecule, the same adsorption pathway will be observed. In the first step, negatively charged metal surface was formed by chloride ions as explained above, following this step the reaction proceeded through formation of $(\text{FeClInh}^+)_{\text{ads}}$ group as a new reaction pathway with equilibrium constant of k_3 (e → f). The positively charged inhibitor molecule will replace Cl⁻ due to more affinity of the hexamine for the metal surface and Cl⁻ is displaced from the metal surface into the solution. Consequently, a new double layer arrangement is formed and metal surface is negatively charges against a positively charged layer of inhibitor molecules $(\text{FeInh}^+)_{\text{ads}}$. The equilibrium constant for the formation reaction of $(\text{FeInh}^+)_{\text{ads}}$ (k_3) is more than k_2 and k_4 , as hexamine molecules have higher affinity towards the metal compared to chloride ions, so the reaction did not stop at this stage (step e) and proceeds further by replacement of Cl⁻ ions.

Effect of hydrodynamic condition: It is important to take into account the flow conditions during corrosion and corrosion inhibition of metals, because flow affects both anodic and cathodic reactions and the inhibitor mass transport. The passive films and inhibitor protective layers are also flow sensitive³⁷. In this study, flow condition is simulated using a rotating disc electrode (RDE). Two electrochemical methods including potentiodynamic polarization and electrochemical impedance spectroscopy (EIS) measurements were performed to study the corrosion of the steel samples in hydrodynamic conditions.

In order to determine whether the flow regime is laminar or turbulent the Reynolds numbers with criterion of $< 10^5$ for laminar flow according to eqn. 10 were calculated.

$$RE = \frac{r^2 \omega}{K_v} \quad (10)$$

In this equation r , ω and K_v are the radius of the RDE active area in mm, angular velocity in rad/s and kinematics viscosity in stokes (mm^2/s), respectively.

Based on the above mentioned criterion for laminar flow, it is clear that the condition is laminar in all the experiments.

Fig. 11 shows polarization curves derived for corrosion of steel specimens in 1M HCl both in static condition and with 200 rpm rotating speed for inhibitor containing solution ($C_{\text{hex}} = 700$ ppm) and the plain solution.

It is obvious that i_{corr} values increase and E_{corr} becomes more positive at higher rotating speeds in both the absence and presence of 700 ppm of hexamine. This behavior for both uninhibited and inhibited solutions shows that the mild steel surface has become nobler in high flow rates, probably due to more non-protective oxide layer formation on the surface.

Fig. 12 depicts the change of charge transfer resistance *versus* rotation speed according to the impedance tests. As can be seen, the R_{ct} values are decreased as the rotation rate increased. Such a trend is in agreement with the increase of I_{corr} with rotation rates, which was previously observed in

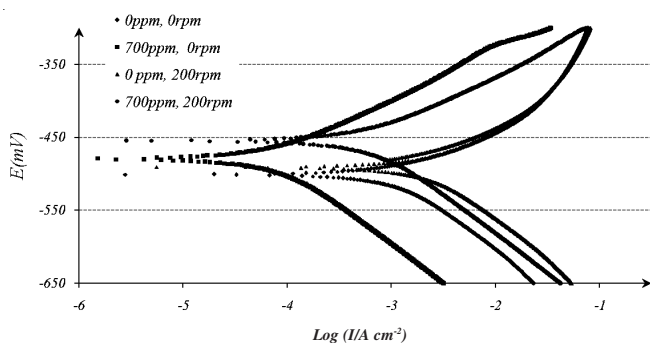


Fig. 11. Polarization curves for mild steel samples in the absence and presence of 700 ppm hexamine in 1M HCl at two different rotation speeds

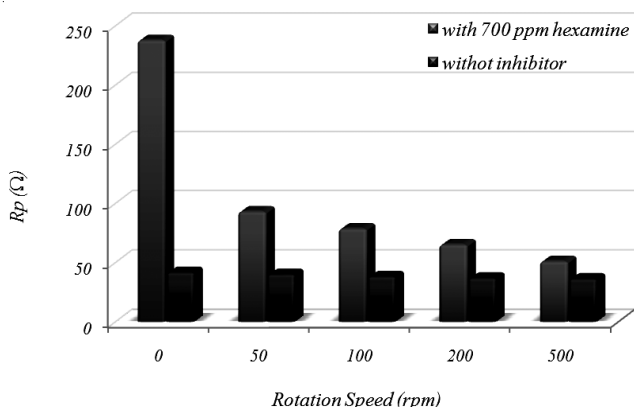
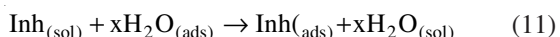


Fig. 12. Effect of hydrodynamic condition on polarization resistance of mild steel specimens in 1M HCl

potentiodynamic polarization measurements. A similar trend is discernible in the presence of inhibitor.

It is generally accepted that the first step in the adsorption of an organic inhibitor on a metal surface usually involves replacement of one or more water molecules adsorbed on the metal surface³⁸:



Based on this model, hydrodynamic conditions can greatly affect the inhibition of metal corrosion, due to the following mechanisms: (i) Flow can increase mass transfer of inhibitor molecules that causes more inhibitor presence at the metal surface. (ii) Hydrodynamic conditions can increase mass transport of metal ions (Fe^{2+}), produced during metal dissolution, from electrode surface to the bulk of the solution. (iii) The high shear stress resulted from high flow velocity can tear apart inhibitor layer or adsorbed (Fe-Inh) complex and cause more desorption from metal surface³⁹.

At low rotation speeds, the shear stress on surface is low. In this condition the rate of Fe^{2+} transfer from surface is higher than the rate of inhibitor transfer to surface and $(\text{Fe-Inh})_{\text{ads}}$ formation. Therefore, adsorption on surface decreases so does the inhibition efficiency. In this way the charge transfer resistance decreases extremely.

Conclusion

The following results can be drawn from this study:

Study on the inhibition mechanism of hexamine revealed that it is a mixed inhibitor in 1M HCl on mild steel.

Activation energies for the corrosion process were calculated as 62.5 kJ mol^{-1} for 1M HCl solution and 85.2 kJ mol^{-1} for 1M HCl solution with 700 ppm of hexamine inhibitor.

Free adsorption energy, enthalpy and entropy of the adsorption of hexamine on mild steel samples in 1M HCl were -31 KJ/mol , -13 KJ/mol and 56 KJ/mol K , respectively. These values are indicative of a physisorption mechanism for the hexamine inhibition.

The results show that the inhibition efficiency was the maximum after 12 h of immersion for the inhibited solution and beyond that immersion time inhibition efficiency declined sharply.

Hydrodynamic condition, contrary to static condition, was deleterious to the inhibition efficiency of hexamine in 1M HCl solution so that there was no adsorption on the surface at rotation speeds higher than 500 rpm.

REFERENCES

- H. Ashassi-Sorkhabi, D. Seifzadeh and M.G. Hosseini, *Corros. Sci.*, **50**, 3363 (2008).
- H. Amar, J. Benzakour, A. Derja, D. Villemin, B. Moreau, T. Braisaz and A. Tounsi, *Corros. Sci.*, **50**, 124 (2008).
- D.-Q. Zhang, Q.-R. Cai, X.-M. He, L.-X. Gao and G.-D. Zhou, *Mater. Chem. Phys.*, **112**, 353 (2008).
- S.A. Abd El-Maksoud, *J. Electroanal. Chem.*, **565**, 321 (2004).
- M. Behpour, S.M. Ghoreishi, M. Salavati-Niasari and B. Ebrahimi, *Mater. Chem. Phys.*, **107**, 153 (2008).
- B. El Mehdi, B. Mernari, M. Traisnel, F. Bentiss and M. Lagrenée, *Mater. Chem. Phys.*, **77**, 489 (2002).
- M.A. Kiani, M.F. Mousavi, S. Ghasemi, M. Shamsipur and S.H. Kazemi, *Corros. Sci.*, **50**, 1035 (2008).
- M. Lagrene'e, B. Mernari, M. Bouanis, M. Traisnel and F. Bentiss, *Corros. Sci.*, **44**, 573 (2002).
- M. Abdallah, *Corros. Sci.*, **45**, 2705 (2003).
- M. Elayyachy, M. Elkodadi, A. Aouniti, A. Ramdanib, B. Hammoutia, F. Malek and A. Elidrissi, *Mater. Chem. Phys.*, **93**, 281 (2005).
- M. Hosseini, S.F.L. Mertens and M.R. Arshadi, *Corros. Sci.*, **45**, 1473 (2003).
- S. Gupta, M. Vajpeyi and S.N. Pandey, *Corros. Prev. Contr.*, **33**, 47 (1986).
- W. Mclead and R.R. Rogers, *Mater. Prot.*, **5**, 28 (1986).
- L.B. Kirilyuk, I.U. Titakova, I.L. Korsunskay and S.P. Miskidzhyan, *Zashch. Metall.*, **16**, 180 (1980).
- D.D.N. Singh, T.B. Singh and B. Gaur, *Corros. Sci.*, **37**, 1005 (1995).
- H.A. El-Dahan, T.Y. Soror and R.M. El-Sherif, *Mater. Chem. Phys.*, **89**, 260 (2005).
- N.I. Podobaev, L.N. Zimova and G.F. Semikolenov, *Zashch. Mefall.*, **13**, 600 (1977).
- S.S. Kirilyuk, A.H. Korsuskaya and S.P. Miskidzhyan, *Zashch. Metall.*, **11**, 197 (1975).
- K. Juttner, *Electrochim. Acta*, **35**, 1501 (1990).
- F.B. Growcock and J.H. Jasinski, *J. Electrochem. Soc.*, **136**, 2310 (1989).
- A.H. Mehaute and G. Grep, *Solid State Ionics*, **9-10**, 17 (1983).
- F. Bentiss, M. Traisnel, L. Gengembre and M. Lagrenée, *Appl. Surf. Sci.*, **152**, 237 (1999).
- E. Naderi, A.H. Jafari, M. Ehteshamzadeh and M.G. Hosseini, *Mater. Chem. Phys.*, **115**, 852 (2009).
- H. Keles, M. Keles, I. Dehri and O. Serindag, *Mater. Chem. Phys.*, **112**, 173 (2008).
- K.F. Khaled, *Mater. Chem. Phys.*, **112**, 290 (2008).
- M.A. Amin, S.S.A. El-Rehim and H.T.M. Abdel-Fatah, *Corros. Sci.*, **51**, 882 (2009).
- S.A.A. El-Maksoud and A.S. Fouda, *Mater. Chem. Phys.*, **93**, 84 (2005).
- S.N. Banerjee, *An Introduction to Science of Corrosion and its Inhibition*, Oxonian Press Pvt. Ltd., India, p. 512.
- S.V. Ramesh and A.V. Adhikari, *Mater. Chem. Phys.*, **115**, 618 (2009).

30. R. Solmaza, G. Kardas, M.C. Ulha, B. Yazici and M. Erbil, *Electrochim. Acta*, **53** (2008).
31. O. Olivares, N.V. Likhanova, B. Gomez, J. Navarrete, M.E. Llanos-Serrano, E. Arce and J.M. Hallen, *Appl. Surf. Sci.*, **252**, 2894 (2006).
32. M.A. Quraishi, I. Ahamad, A.K. Singh, S.K. Shukla, B. Lal and V. Singh, *Mater. Chem. Phys.*, **112**, 1095 (2008).
33. R. Solmaz, G. Kardas, B. Yazic and M. Erbil, *Colloids Surf. A*, **312**, 7 (2008).
34. S.S.A. El-Rehim, M.A.M. Ibrahim and K.F. Khalid, *Mater. Chem. Phys.*, **70**, 268 (2001).
35. M.M. Saleh, *Mater. Chem. Phys.*, **98**, 83 (2006).
36. L. Tang, X. Li, L. Li, G. Mu and G. Liu, *Mater. Chem. Phys.*, **97**, 301 (2006).
37. H. Ashassi-Sorkhabi and E. Asghari, *Electrochim. Acta*, **54**, 162 (2008).
38. G. Kear, B.D. Barker, K.R. Stokes and F.C. Walsh, *Electrochim. Acta*, **52**, 1889 (2007).
39. X. Jiang, Y.G. Zheng and W. Ke, *Corros. Sci.*, **47**, 2636 (2005).